

Article

# Overcoming Water Insolubility in Flow: Enantioselective Hydrolysis of Naproxen Ester

David Roura Padrosa <sup>1</sup>, Valerio De Vitis <sup>2</sup>, Martina Letizia Contente <sup>1,\*</sup>, Francesco Molinari <sup>2</sup> and Francesca Paradisi <sup>1,\*</sup>

<sup>1</sup> School of Chemistry, University of Nottingham, University Park, Nottingham NG7 2RD, UK; david.roura@nottingham.ac.uk

<sup>2</sup> Department of Food, Environmental and Nutritional Sciences (DeFENS), Università degli studi di Milano, Via Mongiagalli 25, 20133 Milan, Italy; valerio.devitis@unimi.it (V.D.V.); francesco.molinari@unimi.it (F.M.)

\* Correspondence: martina.contente@nottingham.ac.uk (M.L.C.); francescaparadisi@nottingham.ac.uk (F.P.); Tel.: +44(0)1159513516 (M.L.C.); +44(0)1157486267 (F.P.)

Received: 6 February 2019; Accepted: 18 February 2019; Published: 3 March 2019



**Abstract:** Hydrolytic enantioselective cleavage of different racemic non-steroidal anti-inflammatory drugs (NSAIDs) ester derivatives has been studied. An engineered esterase form *Bacillus subtilis* (BS2m) significantly outperformed homologous enzymes from *Halomonas elongata* (HeE) and *Bacillus coagulans* (BCE) in the enantioselective hydrolysis of naproxen esters. Structural analysis of the three active sites highlighted key differences which explained the substrate preference. Immobilization of a chimeric BS2m-T4 lysozyme fusion (BS2mT4L1) was improved by resin screening achieving twice the recovered activity ( $22.1 \pm 5$  U/g) with respect to what had been previously reported, and was utilized in a packed bed reactor. Continuous hydrolysis of  $\alpha$ -methyl benzene acetic acid butyl ester as a model substrate was easily achieved, albeit at low concentration (1 mM). However, the high degree of insolubility of the naproxen butyl ester resulted in a slurry which could not be efficiently bioconverted, despite the addition of co-solvents and lower substrate concentration (1 mM). Addition of Triton<sup>®</sup> X-100 to the substrate mix yielded 24% molar conversion and 80% e.e. at a 5 mM scale with 5 min residence time and sufficient retention of catalytic efficiency after 6 h of use.

**Keywords:** esterases; flow biocatalysis; enzyme immobilization; surfactants; NSAIDs

## 1. Introduction

Non-steroidal anti-inflammatory drugs (NSAIDs) are a group of propionic acid derivatives which inhibit the cyclooxygenase (COX). Although normally commercialized as racemic mixtures, the specific biological effect of these drugs is closely linked to their chirality [1–3].

Carboxylic ester hydrolases (EC 3.1.1.X) belong to a large group of enzymes that catalyze the cleavage or formation of ester bonds. Carboxylesterases (EC 3.1.1.1) and lipases (EC 3.1.1.3), classified based on their substrate specificity [4] are two different classes of hydrolytic enzymes, however, the architecture of the hydrolases active site is highly conserved even among enzymes catalyzing different reactions [5]. Thanks to their ability to stereoselectively hydrolyze or form esters they can be applied to the preparation of NSAIDs [6,7].

Taking advantage of the lipase's high resistance to organic media, the enantiopure preparation of NSAIDs has been reported mainly by esterification with free or immobilized lipases in organic solvents to overcome the poor solubility of such substrates in water [6–9]. More recently, Novozym435, a commercially available immobilized lipase form *Candida Antarctica* (CALB), was applied in a flow reactor for the continuous preparation of flurbiprofen in toluene [10]. However, conversion

rates of these reactions are negatively affected by the presence of water, impacting consequently on their scalability.

On the other hand, the stereoselective hydrolysis of NSAID's esters can be performed in aqueous solutions, yielding directly the active drug which contains the free carboxylic acid, and thus, their scale up would be less problematic. Esterase catalyzed hydrolysis of racemic NSAIDs has been tested using both soluble and immobilized enzymes [11–13]. However, very few examples are available on the bio-catalyzed hydrolysis in a continuous flow reactors due to two main reasons: (1) the challenging covalent-immobilization of esterases [14] and (2) the low water solubility of NSAIDs acid and its esters derivatives in water [15]. The implementation of flow chemistry for insoluble substrates is severely limited [16] due to possible blockages of the reactor, poor contact time with heterogeneous immobilized catalysts, and low mass transfer. Where possible, solubility can be improved with the addition of a co-solvent or the use of two-liquid phase systems [17,18]. These systems, however, rely on the resistance of the biocatalyst to the organic solvent chosen and the partitioning of the substrate in the two-phase set up, and, while in some cases they are beneficial for the separation of the product from the substrate, this does not always apply if the solubility does not differ significantly.

In the present study, the enantioselective cleaving of naproxen and other NSAIDs ester derivatives with three different esterases was studied. BS2m from *Bacillus subtilis* and BCE from *Bacillus coagulans* were previously described [19–21], while HeE from *Halomonas elongata* is a novel enzyme. A comparison between the three active site architectures, paying particular attention to the tunnel leading to the catalytic site, has been reported. Moreover, the immobilization of a chimeric BS2m-T4 lysozyme fusion (BS2mT4L1) [22], was optimized. The use of surfactants to address solubility issues for flow applications was also explored.

## 2. Results

### 2.1. NSAID Hydrolysis

To better understand the applicability of carboxyl esterases for the hydrolysis of NSAIDs, three homologous enzymes were used for comparison. BS2m, an engineered versatile esterase from *Bacillus subtilis* [19,20], BCE from *Bacillus coagulans* with a mini-lid similarly to the one found in lipases [21] and HeE, a new esterase cloned from the halotolerant bacteria *Halomonas elongata* (Figure S1).

Following initial screening, HeE exhibited more activity against butyl esters (Table S1) similarly to BS2m previously reported to have a better activity with *p*-nitrophenyl butyrate [19]. BCE, on the other hand, had its maximum activity with ethyl esters [21]. Consequently, their ability to cleave NSAIDs derivative was assessed with butyl esters for the first two and with ethyl esters for BCE.

The results of the batch hydrolysis of 10 mM substrate (1a–1c) are shown in Table 1. BS2m and HeE achieved almost complete conversion with ibuprofen and flurbiprofen butyl ester over 8 h and 24 h, respectively. Both enzymes lacked any stereo-preference even at shorter reaction times. BCE on the other hand gave its best results after 24 h yielding 22% and a 36% of the (*S*)-ibuprofen and (*S*)-flurbiprofen, respectively (>97% e.e.). Naproxen behaved differently; BCE was completely unable to hydrolyze the substrate, while both HeE and BS2m achieved moderate conversion after 48 h (35% and 55%, respectively) however, BS2m displayed a significant degree of enantioselectivity (80% e.e. (*R*)-enantiomer, after 48 h with a conversion yield of 55%).

**Table 1.** Maximum molar conversion (m.c.) and enantiomeric excess (e.e.) of the batch biotransformations with all three enzymes and the substrates tested. A general scheme of the hydrolysis reaction is shown. For conversions <5% e.e. could not be detected (n.d). All enzymes were used at 0.1 mg/mL.

	Substrate	BCE <sup>1</sup>		HeE <sup>2</sup>		BS2m <sup>2</sup>	
		m.c.	e.e.	m.c.	e.e.	m.c.	e.e.
1a.	Naproxen Ester	<5% (48 h)	n.d.	35% (48 h)	<5%	55% (48 h)	80% (R)
1b.	Ibuprofen ester	22% (24 h)	>97% (S)	>95% (8 h)	<5%	>95% (8 h)	<5%
1c.	Flurbiprofen ester	36% (24 h)	>97% (S)	88% (24 h)	<5%	81% (24 h)	<5%

<sup>1</sup> Substrates used were R<sub>1</sub> ethyl esters; <sup>2</sup> Substrates used were R<sub>1</sub> butyl esters.

## 2.2. Active Site and Tunnel Architecture

The architecture of the catalytic site and its proximities was probed by in-silico modeling to explain the different capability of accepting highly bulky substrates with low molecular flexibility such as naproxen. For both BS2m and HeE, models created with IntFold were used [23]. For BCE, the crystal structure of open-lid conformation was used (PDB: 5OLU).

The catalytic triad was identical for the three esterases in terms of nature and positioning of the residues in the 3-dimensional structure. All three enzymes showed a similar positioning of the catalytic residues, and no notable difference was observed in the surrounding environment (see Figure 1). However, the geometry and biochemical characteristics of the tunnel leading to the active site [24], which was analyzed using Caver in a static structure [25], shown in Figure 2, were more revealing.

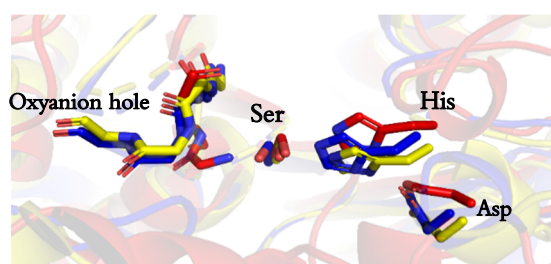


**Figure 1.** Active site details of the three esterases. *Bacillus coagulans* (BCE), represented in red, *Halomonas elongata* (HeE) in blue, and *Bacillus subtilis* (BS2m) represented in yellow. The active triad as well as the residues forming the oxyanion hole is presented.

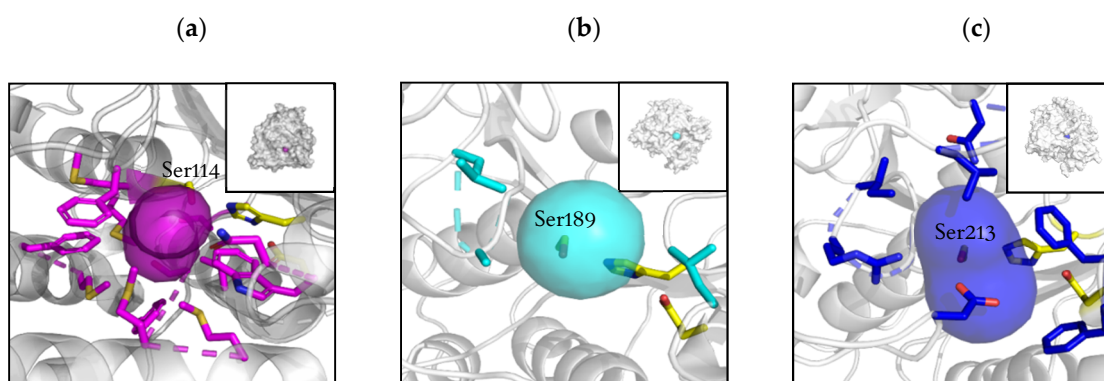


**Figure 2.** Graphic representation of the tunnel leading to the active site. The catalytic triad is showed in yellow and the residues participating in the tunnel in pink for BCE (a), light blue for BS2m (b) and dark blue for HeE (c). The catalytic serine is labelled in all structures.

From the different tunnels computed and predicted by the program, the shortest and with less restrictive bottleneck was chosen. BS2m predicted tunnel was less than 2 Å, and located very superficially in the protein, allowing easy access for any substrate. For HeE, the length increased more than three times, and for BCE the computed length was more than 10 Å (Table S2). Both tunnels of HeE and BCE showed bottlenecks of less than 2 Å and a curvature, suggesting serious impediments for non-flexible substrates to reach the active site. Moreover, the residues surrounding these entrances appear to be significant for substrate recognition and shuttling in HeE and BCE. The BCE tunnel is formed by 60% of hydrophobic chain amino acids, with Phe38 and Trp190 creating the 1.29 Å bottleneck. This two residues could act as a gate as previously seen for acetylcholine esterases [26]. For HeE, the entrance is less constricted, with no obvious bottleneck and with the presence of residues with a charged side-chain (Arg132, Asp288 and Glu327).

All together, these differences could explain the poor activity of HeE and BCE behavior towards bulky, rigid substrates as naproxen esters. HeE showed some hydrolytic activity as its tunnel is more flexible and prone to shuttle, allowing naproxen butyl ester to enter the catalytic site with less effort than BCE for the corresponding ethyl ester.

### 2.3. Immobilization of BS2mT4L1 and Flow Assisted Hydrolysis of Naproxen Butyl Ester

In order to exploit the hydrolysis of naproxen in flow, BS2m was chosen as it showed the highest activity and selectivity. Covalent immobilization of esterases is generally problematic, resulting in low recovered activity, as they tend to form a superficial layer on the carrier, hindering the substrate diffusion [27,28]. We previously reported on the immobilization of a fusion protein of BS2m with the T4 lysozyme (BS2mT4L1) on an epoxy derivatized methacrylate support (EC-403), which yielded a biocatalyst with a comparable activity ( $6.2 \pm 0.8$  U/g) to *Candida albicans* lipase B, most used and known as (CALB), using 16 times less enzyme [22].

To improve further the performance of the immobilized catalyst, higher catalyst loading was tested. With a loading of 7.5 mg/g of resin, the biocatalyst displayed an activity of  $11 \pm 2$  U/g with respect to  $6.2 \pm 0.8$  obtained previously. However, when this catalyst was tested in flow with  $\alpha$ -methyl-benzene acetic acid butyl ester ( $\alpha$ MBBE; 1d) as a model substrate, no conversion was observed. An upstream inlet of toluene (Figure 3a) allowed the recovery of the ester moiety, but no hydrolysis occurred. Moreover, the presence of toluene affected dramatically the stability of the immobilized biocatalyst, with only 25% of the initial activity after five cycles. Immobilization on a less hydrophobic methacrylate resin (Relysorb<sup>®</sup> HG400) as well as on epoxy-functionalized agarose CL6B (Ag-ep) [29] was trialed to increase hydrophilicity of the matrix while retaining the immobilization chemistry. Both strategies yielded a biocatalyst with almost twice the activity of EP403-BS2mT4L1 (HG400-BS2mT4L1:  $21 \pm 3$  U/g; Ag-ep-BS2mT4L1:  $22.1 \pm 5$  U/g), however HG400-BS2mT4L1 in

flow performed as the EC-403 preparation failing to convert the substrate. On the other hand, Ag-ep-BS2mT4L1 yielded 40% product with  $\alpha$ MBBE (1 mM).

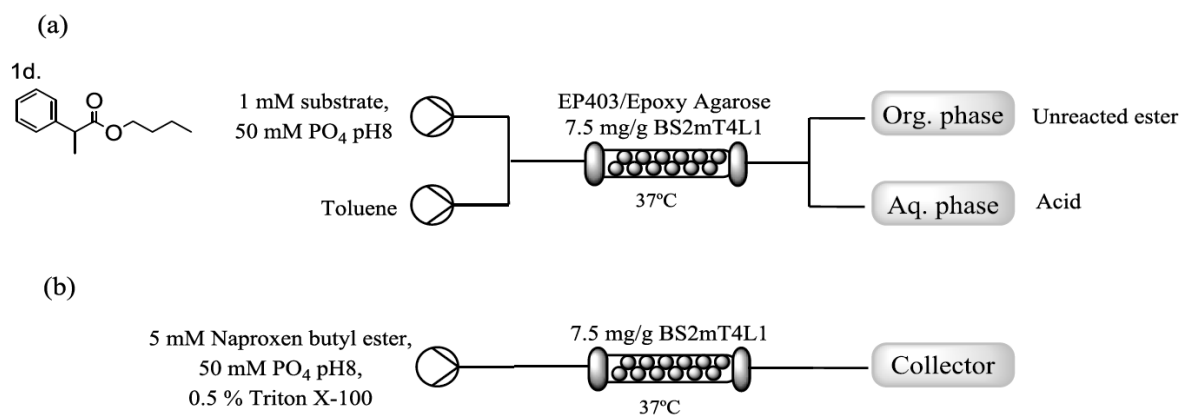


**Figure 3.** (a) Scheme of the setup of the flow reactor with toluene and (b) outline of the final setup for the enantioselective hydrolysis of naproxen.

However, when naproxen was tested under the same conditions, this did not lead to any product formation. It is important to note that while  $\alpha$ MBBE appeared as a clear solution, naproxen butyl ester, even at 1 mM, is a suspension due to its highly hydrophobic nature. Suspensions, while they can be used with a peristaltic pump system, could still potentially block the pump lines and the interaction between the heterogenous biocatalyst and the particles is more challenging. A range of water-miscible organic solvents (ethanol, methanol, DMSO and acetonitrile up to 20%) were tested in order to solubilize the naproxen ester with no improvement. The use of surfactants in batch reactions involving free enzymes and highly hydrophobic molecules such as profen esters had been reported to enhance both the relative activity of the biocatalyst and the solubilization of the substrate but no previous examples in flow or with immobilized catalyst is known. Triton<sup>®</sup> X-100, a nonionic surfactant, showed the highest increase in the reaction rate without affecting the enantioselectivity using an esterase from *Pseudomonas sp.* [12]. In this study, Triton<sup>®</sup> X-100 was added to the naproxen ester suspension in low concentration, 0.5% (*v/v*), to minimize the distortion of the enzymatic structure and effect on the activity [30,31], while improving naproxen butyl ester solubility. Under this conditions, complete solubility of 1 and even 5 mM solution of naproxen butyl ester was achieved.

The surfactant enriched solution was applied in flow (Figure 3b) and the results are presented in Table 2. Complete cleavage of the ester was observed within 30 min, while the batch reaction yielded only a 55% conversion over 48 h. Moreover, since BS2m showed selectivity for the (R)-enantiomer in the batch reactions, the retention time was shortened to see if a degree of enantiopreference could be achieved. With 10 min residence time the conversion diminished to 65% but an e.e. of 40% was obtained. Reducing further the residence time to 6 min the enantiomeric excess increased to 80% while the conversion was 24%. The activity of the biocatalyst was then checked to assess the effect of Triton<sup>®</sup> X-100 on its stability. After a total working time of six hours at a constant flow rate of 0.117 mL/min, the biocatalyst retained still 57% of activity ( $12.5 \pm 1$  U/g).

**Table 2.** Flow assisted hydrolysis of naproxen butyl ester. The substrate was prepared in 50 mM phosphate buffer pH 8 with 5% DMSO and 0.5% of Triton<sup>®</sup> X-100. All reactions were performed at 37 °C.

Naproxen Butyl Ester Concentration (mM)	Residence Time (minutes)	Molar Conversion (%)	e.e. (%)
1 mM	30	>99%	<5%
	30	>99%	<5%
5 mM	10	65%	40%
	6	24%	80%

### 3. Discussion

A comparative study of three different carboxylesterases, BCE, HeE and BS2m, highlighted differences in the ability to hydrolyze NSAID's esters. These could be partially explained by the architecture of their tunnel leading to the active site. BS2m was significantly more active against naproxen as the active site was more solvent exposed. In contrast, BCE presented a mini-lid structure while HeE had the N-terminal  $\alpha$ -helix partially covering the entrance to the active site. These two structural features resulted in longer tunnels leading to the active site making the catalysis of non-flexible substrates more challenging.

The immobilization of BS2mT4L1, previously reported, was enhanced by higher enzyme loading and using a more hydrophilic matrix such as Relysorb<sup>®</sup> HG400 and agarose CL6B which lead to a catalyst with 22 U/g of activity which almost doubled what was achieved with polymethacrylate beads such as Relyzime<sup>®</sup> EC-403. The resulting biocatalyst was successfully applied in a packed bed reactor for the continuous flow enantioselective hydrolysis of naproxen.

With the shorter retention time, a molar conversion of 24% and 80% e.e. was obtained. Therefore, this exemplifies an enantioselective cleaving in mild conditions and buffered system with the use of Triton<sup>®</sup> X-100 as a surfactant. The presence of Triton<sup>®</sup> X-100 helps to solubilize a highly hydrophobic substrate such as naproxen butyl ester. Moreover, the biocatalyst showed a good operational stability after 6 h, with 57% of retained activity.

In conclusion, the combination of a better immobilization strategy and the use of surfactant to enhance the solubility of naproxen butyl ester enables the enantioselective hydrolysis. Finally, the biocatalyst exhibited good stability in those conditions.

### 4. Materials and Methods

#### 4.1. *Halomonas elongata* (HeE) Cloning

HELO\_2889 was identified as a putative carboxylic-ester hydrolase by homology search using *Bacillus subtilis* esterase para-nitrobenzyl esterase (PDB: 1QE3) and *Bacillus coagulans* (BCE) (PDB: 5OLU). The gene was amplified from *Halomonas elongata* DSM 2581 genome with the following primers: 5'-CCC TGT GCG GGATCC TGA CGT CAT GCG CAA AGC TCA AGC 3' and 5'-ATA TAA A GGTACC CAT CAG TTG ATC TGC AGG CTG TCC AGC GAC G-3' using a Touchdown PCR protocol. Primers were designed to incorporate a BamHI and KpnI restriction site respectively (underlined). The amplified gene was cloned into a pRSET-b plasmid and transformed into chemically competent *E. coli* BL21 (DE3) pLysS.

#### 4.2. BS2m, HeE and BCE Production

BCE and *Bacillus subtilis* (BS2m) were expressed as previously described [19–21]. For HeE, *E. coli* BL21(DE3) pLysS-HeE was grown at 37 °C, 180 rpm in Terrific Broth media supplemented with ampicillin (100  $\mu$ g/mL) until the OD600 reached 0.6–0.8. Before the addition of 0.5 mM IPTG, the culture was incubated in ice for 30 min, to enhance the expression as done with BCE, and subsequently

grown for an additional 20 h at 30 °C, 180 rpm. Cells were harvested by centrifugation (4500 rpms, 20 min) and resuspended in an appropriate volume of 50 mM potassium phosphate buffer pH 8. 1 mg/mL of lysozyme (Sigma Aldrich) was added, and the mixture stirred for 15 min at 37 °C, 180 rpm. After sonication (10 cycles 1 min on and 1 min off), cell debris were removed by centrifugation (1 h at 4 °C, 14,000 rpm). HeE was then purified by IMAC chromatography using an ÄKTA pure UPLC (loading buffer: 50 mM potassium phosphate buffer, 0.3 M NaCl, 30 mM imidazole, pH 8; elution buffer: 50 mM potassium phosphate buffer, 0.3 M NaCl, 300 mM imidazole, pH 8). The fractions containing the pure protein were dialyzed against 50 mM potassium phosphate buffer pH 8 overnight.

#### 4.3. Esterase Activity Assay

For the free enzymes, the activity was measured spectrophotometrically at 420 nm by determining the formation of para-nitrophenol at 25 °C in half-microcuvette (total volume 1 mL) for 5 min, taking a measurement every 30 seconds. The reference conditions were 0.5 mM para-nitro phenylacetate (pNPA; stock solution: 100 mM in acetone) 50 mM potassium phosphate buffer, pH 8. ( $\epsilon = 15000 \text{ M}^{-1} \text{ cm}^{-1}$ ).

BS2m had an activity of 61 U/mg, BS2mT4L1 of 32 U/mg, HeE of 3.5 U/mg and BCE an activity of 0.03 U/mg against pNPA.

One unit (U) of activity is defined as the amount of enzyme which catalyzes the consumption of 1  $\mu\text{mol}$  of para-nitrophenyl acetate per minute under reference conditions.

For the immobilized enzyme, activity was measured using 25–50 mg of resin in an appropriate volume (10–20 mL) in the reference conditions. The solution was kept at 30 °C with shaking and the absorbance was measured every minute for 10 minutes.

#### 4.4. Butyl-Ester NSAID's Synthesis

A solution of racemic or enantiopure acid (250 mg, 1 eq), butanol (1.5 eq) and 4-dimethylaminopyridine (DMAP 0.12 eq) in  $\text{CH}_2\text{Cl}_2$  (10 mL), was cooled down and 1.1 eq of dicyclohexylcarbodiimide (DCC) were added. The reaction was monitored by TLC (9:1 *n*-hexane/ethyl acetate) and once completed, filtered and washed with 5 mL of  $\text{CH}_2\text{Cl}_2$ . The crude was then purified by flash chromatography (9:1 *n*-hexane/ethyl acetate). All synthesized molecules' purity was checked by HPLC and NMR (see Methods S1).

#### 4.5. Batch Biotransformations with Free Enzymes

Biotransformations were performed with 10 mM suspensions of the corresponding ester derivative and 0.1 mg/mL of enzyme in 50 mM potassium phosphate buffer pH 8 with 10% DMSO as cosolvent. Samples of 100  $\mu\text{L}$  were withdrawn at different times and the reaction was quenched by adding 450  $\mu\text{L}$  of HCl 0.2% and 450  $\mu\text{L}$  of acetonitrile. The samples were analyzed by HPLC (Dionex UltiMate 3000, Waters X-Bridge C18 (3.5  $\mu\text{m}$ , 2.1  $\times$  100 mm), 0.8 mL/min, measuring at 210 nm, 250 nm and 265 nm) to assess the conversion. The retention times in minutes were:  $\alpha$ -methyl benzyl acetic acid butyl ester 5.47,  $\alpha$ -methyl benzyl acetic acid 3.98, flurbiprofen butyl ester 5.98, flurbiprofen acid 4.86, ibuprofen butyl ester 6.22, ibuprofen acid 5.05, naproxen butyl ester 5.74, naproxen acid 4.52.

#### 4.6. HPLC Analysis to Determine the Enantioselectivity

HPLC analyses were performed with a Jasco PU-980 pump equipped with a UV-vis detector Jasco UV-975 (wavelength: 254 nm). Column: Lux Amylose-2, 4.60 mm i.d.  $\times$  150 mm, Phenomenex. Eluent: acetonitrile:water:formic acid (1:1:0.2, *v/v/v*). Flow: 1.0 mL/min. Retention times: (R)-Flurbiprofen 4.3 min; (S)-Flurbiprofen 5.7 min; (R)-Flurbiprofen ethyl ester 28.2 min; (S)-Flurbiprofen ethyl ester 36.1 min; (R)-Flurbiprofen butyl ester 29.8 min; (S)-Flurbiprofen butyl ester 37.8 min. Column Lux Cellulose-3, 4.60 mm i.d.  $\times$  150 mm, Phenomenex. Eluent *n*-hexane:2-propanol:formic acid (98:2:0.1, *v/v/v*). Flow: 1.0 mL/min. Retention times: (R)-Ibuprofen butyl ester 4.0 min; (S)-Ibuprofen butyl ester 4.6 min; (R)-Ibuprofen ethyl ester 4.3 min; (S)-Ibuprofen ethyl ester 5.0 min; (R)-Ibuprofen 7.9 min; (S)-Ibuprofen ethyl ester 8.7 min. Column Lux Cellulose-1, 4.60 mm i.d.  $\times$  150 mm, Phenomenex. Eluent

*n*-hexane:2-propanol:formic acid (92:8:0.1, *v/v/v*). Flow: 1.0 mL/min. Retention times: (*R*)-Naproxen butyl ester 5.0 min; (*S*)-Naproxen butyl ester 6.1 min; (*R*)-Naproxen ethyl ester 5.6 min; (*S*)-Naproxen ethyl ester 6.5 min; (*R*)-Naproxen 10.5 min; (*S*)-Naproxen 11.2 min.

#### 4.7. Computational Analysis of Tunnels

The analysis of the tunnel leading to the catalytic site of the different esterases was performed using CAVER 3.0 plugin for Pymol [25] selecting as endpoint the catalytic serine. When available, crystal structures of the proteins were used, or homology models were created using the IntFold server [23].

#### 4.8. Preparation of Agarose with Epoxide Groups

Preparation of agarose with epoxide groups (Ag-ep) was prepared and the quantification of epoxide was conducted as described before [29]. In all batches, the resin contained  $60 \pm 4$   $\mu$ mol of epoxides/g of dry resin.

#### 4.9. Immobilization of BS2mT4L1 in Epoxy-Agarose

BS2mT4L1 immobilization was optimized from Planchestainer et al. [22]. One gram of the previously prepared Ag-ep was mixed with 2 mL of modification buffer (1 M Sodium borate, 2 M iminodiacetic acid in 50 mM phosphate buffer Ph 8.5) and left shaking at room temperature for 2 h. The mixture was filtered under vacuum and washed with abundant H<sub>2</sub>O before the addition of 5 mL of metal buffer (1M NaCl, 45 mM CoCl<sub>2</sub> in 50 mM phosphate buffer pH 6) and left to agitate for 2 h.

Following vacuum filtration and washing with H<sub>2</sub>O, the desired amount of protein was added and left shaking overnight at room temperature. The mixture was then filtered under vacuum and 3 mL of desorption buffer (50 mM EDTA, 0.5 M NaCl in 20 mM phosphate buffer pH 7.2) were added to eliminate the metal before the addition of blocking buffer (3 M glycine in 50 mM phosphate buffer pH 8.5). The mixture was left shaking for 20 h and finally filtered and washed with H<sub>2</sub>O and the biocatalyst was kept in 50 mM phosphate buffer pH 8.

#### 4.10. Flow Reactions

Flow reaction were performed using a R2+/R4 flow reactor from Vapourtec using an Omnifit glass column (6.6 mm  $\times$  100 mm length) filled with 10.2 g of biocatalyst for the longest residence time. Initially, a solution of the substrate was prepared in 50 mM phosphate buffer with 10% DMSO. When needed, the solution was mixed in a T-tube with toluene (2:1) upstream of the packed column.

For the resolution of racemic naproxen butyl ester, 5 mM of Naproxen butyl ester was prepared in 50 mM phosphate buffer with 0.5% (*v/v*) of Triton<sup>®</sup> X-100.

The flow rate was varied and optimized. Molar conversion and enantiomeric excess were assessed by HPLC as previously described.

**Supplementary Materials:** The following are available online at <http://www.mdpi.com/2073-4344/9/3/232/s1>, Figure S1: SDS-gel of the purification of HeE, Table S1: kinetic parameters of HeE for *para*-nitrobenzyl acetate and *para*-nitrobenzyl butyrate, Table S2: physical parameters of the calculated tunnels for BCE, BS2m and HeE, Methods S1: NMR characterization of NSAIDs butyl esters.

**Author Contributions:** D.R.P., M.L.C. and F.P. designed the study. D.R.P. cloned HeE, immobilized and evaluated BS2mT4L1, synthesized the substrates and performed the flow reactions and the HPLC analysis. V.D.V. and M.L.C. performed the biotransformations with BCE and performed the HPLC analysis. D.R.P., M.L.C. and F.P. wrote the paper. F.M. and F.P. supervised the work. All the authors discussed the results and commented on the manuscript.

**Funding:** This work was supported by the Biotechnology and Biological Research Council [grant number BB/P002536/1] and the European Union's Horizon 2020 Research and Innovation Programme under the Marie Skłodowska-Curie grant agreement N. 792804\_AROMAs-FLOW (M.L.C.).

**Acknowledgments:** The authors wish to thank Resindion S.R.L. for donating Relyzime<sup>®</sup> EP403/S and Relysorb<sup>®</sup> HG400 and Uwe Bornscheuer for providing BS2m plasmid.



**Conflicts of Interest:** The authors declare no conflict of interest.

## References

1. Hayball, P.J.; Hayball, D.P. Chirality and Nonsteroidal Anti-Inflammatory Drugs. *Drugs* **1996**, *52*, 47–58. [[CrossRef](#)] [[PubMed](#)]
2. Wynne, S.; Djakiew, D. NSAID Inhibition of Prostate Cancer Cell Migration Is Mediated by Nag-1 Induction via the p38 MAPK-p75NTR Pathway. *Mol. Cancer Res.* **2010**, *8*, 1656–1664. [[CrossRef](#)] [[PubMed](#)]
3. Harrison, I.T.; Lewis, B.; Nelson, P.; Rooks, W.; Roszkowski, A.; Tomolonis, A.; Fried, J.H. Nonsteroidal antiinflammatory agents. I. 6-Substituted 2-naphthylacetic acids. *J. Med. Chem.* **1970**, *13*, 203–205. [[CrossRef](#)] [[PubMed](#)]
4. Arpigny, J.L.; Jaeger, K.-E. Bacterial lipolytic enzymes: classification and properties. *Biochem. J.* **1999**, *343*, 177. [[CrossRef](#)] [[PubMed](#)]
5. Lenfant, N.; Hotelier, T.; Velluet, E.; Bourne, Y.; Marchot, P.; Chatonnet, A. ESTHER, the database of the  $\alpha/\beta$ -hydrolase fold superfamily of proteins: tools to explore diversity of functions. *Nucleic Acids Res.* **2012**, *41*, D423–D429. [[CrossRef](#)] [[PubMed](#)]
6. Chang, C.-S.; Hsu, C.-S. Lipase-catalyzed enantioselective esterification of (S)-naproxen hydroxyalkyl ester in organic media. *Biotechnol. Lett.* **2003**, *25*, 413–416. [[CrossRef](#)] [[PubMed](#)]
7. Ong, A.; Kamaruddin, A.; Bhatia, S.; Long, W.; Lim, S.; Kumari, R. Performance of free *Candida antarctica* lipase B in the enantioselective esterification of (R)-ketoprofen. *Enzyme Microb. Technol.* **2006**, *39*, 924–929. [[CrossRef](#)]
8. Chen, J.-C.; Tsai, S.-W. Enantioselective Synthesis of (S)-Ibuprofen Ester Prodrug in Cyclohexane by *Candida rugosa* Lipase Immobilized on Accurel MP1000. *Biotechnol. Progress* **2000**, *16*, 986–992. [[CrossRef](#)] [[PubMed](#)]
9. Yousefi, M.; Mohammadi, M.; Habibi, Z. Enantioselective resolution of racemic ibuprofen esters using different lipases immobilized on octyl sepharose. *J. Mol. Catal. B Enzym.* **2014**, *104*, 87–94. [[CrossRef](#)]
10. Tamborini, L.; Romano, D.; Pinto, A.; Bertolani, A.; Molinari, F.; Conti, P. An efficient method for the lipase-catalysed resolution and in-line purification of racemic flurbiprofen in a continuous-flow reactor. *J. Mol. Catal. B Enzym.* **2012**, *84*, 78–82. [[CrossRef](#)]
11. Quax, W.J.; Broekhuizen, C.P. Development of a new *Bacillus* carboxyl esterase for use in the resolution of chiral drugs. *Appl. Microbiol. Biotechnol.* **1994**, *41*, 425–431. [[CrossRef](#)] [[PubMed](#)]
12. Lee, E.G.; Won, H.S.; Ro, H.-S.; Ryu, Y.-W.; Chung, B.H. Preparation of enantiomerically pure (S)-flurbiprofen by an esterase from *Pseudomonas* sp. KCTC 10122BP. *J. Mol. Catal. B Enzym.* **2003**, *26*, 149–156. [[CrossRef](#)]
13. Steenkamp, L.; Brady, D. Screening of commercial enzymes for the enantioselective hydrolysis of *R,S*-naproxen ester. *Enzyme Microb. Technol.* **2003**, *32*, 472–477. [[CrossRef](#)]
14. A Sousa, H.; Rodrigues, C.; Klein, E.; Afonso, C.A.M.; Crespo, J.G. Immobilisation of pig liver esterase in hollow fibre membranes. *Enzyme Microb. Technol.* **2001**, *29*, 625–634. [[CrossRef](#)]
15. Fini, A. Solubility and solubilization properties of non-steroidal anti-inflammatory drugs. *Int. J. Pharm.* **1995**, *126*, 95–102. [[CrossRef](#)]
16. Hopkin, M.D.; Baxendale, I.R.; Ley, S.V. An expeditious synthesis of imatinib and analogues utilising flow chemistry methods. *Org. Biomol. Chem.* **2013**, *11*, 1822–1839. [[CrossRef](#)] [[PubMed](#)]
17. Baxendale, I.R. The integration of flow reactors into synthetic organic chemistry. *J. Chem. Technol. Biotechnol.* **2013**, *88*, 519–552. [[CrossRef](#)]
18. Tamborini, L.; Fernandes, P.; Paradisi, F.; Molinari, F. Flow Bioreactors as Complementary Tools for Biocatalytic Process Intensification. *Trends Biotechnol.* **2018**, *36*, 73–88. [[CrossRef](#)] [[PubMed](#)]
19. Schmidt, M.; Henke, E.; Heinze, B.; Kourist, R.; Hidalgo, A.; Bornscheuer, U.T. A versatile esterase from *Bacillus subtilis*: Cloning, expression, characterization, and its application in biocatalysis. *Biotechnol. J.* **2007**, *2*, 249–253. [[CrossRef](#)] [[PubMed](#)]
20. Hackenschmidt, S.; Moldenhauer, E.J.; Behrens, G.A.; Gand, M.; Pavlidis, I.V.; Bornscheuer, U.T. Enhancement of Promiscuous Amidase Activity of a *Bacillus subtilis* Esterase by Formation of a  $\pi$ - $\pi$  Network. *ChemCatChem* **2013**, *6*, 1015–1020. [[CrossRef](#)]
21. De Vitis, V.; Nakhnoukh, C.; Pinto, A.; Contente, M.L.; Barbiroli, A.; Milani, M.; Bolognesi, M.; Molinari, F.; Gourlay, L.J.; Romano, D. A stereospecific carboxyl esterase from *Bacillus coagulans* hosting nonlipase activity within a lipase-like fold. *FEBS J.* **2018**, *285*, 903–914. [[CrossRef](#)] [[PubMed](#)]

22. Planchestainer, M.; Padrosa, D.R.; Contente, M.; Paradisi, F. Genetically Fused T4L Acts as a Shield in Covalent Enzyme Immobilisation Enhancing the Rescued Activity. *Catalysts* **2018**, *8*, 40. [[CrossRef](#)]
23. McGuffin, L.J.; Atkins, J.D.; Salehe, B.R.; Shuid, A.N.; Roche, D.B.; Pérez-Berná, A.J.; Marion, S.; Chichón, F.J.; Fernández, J.J.; Winkler, D.C.; et al. IntFOLD: An integrated server for modelling protein structures and functions from amino acid sequences. *Nucleic Acids Res.* **2015**, *43*, W169–W173. [[CrossRef](#)] [[PubMed](#)]
24. Kingsley, L.J.; Lill, M.A. Substrate tunnels in enzymes: Structure-function relationships and computational methodology. *Proteins* **2015**, *83*, 599–611. [[CrossRef](#)] [[PubMed](#)]
25. Pavelka, A.; Sebestova, E.; Kozlikova, B.; Brezovský, J.; Sochor, J.; Damborsky, J. CAVER: Algorithms for Analyzing Dynamics of Tunnels in Macromolecules. *IEEE/ACM Trans. Comput. Biol. Bioinf.* **2016**, *13*, 1. [[CrossRef](#)] [[PubMed](#)]
26. Gora, A.; Brezovsky, J.; Damborsky, J. Gates of enzymes. *Chem. Rev.* **2013**, *113*, 5871–5923. [[CrossRef](#)] [[PubMed](#)]
27. Sheldon, R.A. Enzyme Immobilization: The Quest for Optimum Performance. *Adv. Synth. Catal.* **2007**, *349*, 1289–1307. [[CrossRef](#)]
28. Ren, H.; Xing, Z.; Yang, J.; Jiang, W.; Zhang, G.; Tang, J.; Li, Q. Construction of an Immobilized Thermophilic Esterase on Epoxy Support for Poly( $\epsilon$ -caprolactone) Synthesis. *Molecules* **2016**, *21*, 796. [[CrossRef](#)] [[PubMed](#)]
29. Mateo, C.; Bolivar, J.M.; Godoy, C.A.; Rocha-Martín, J.; Pessela, B.C.; Curiel, J.A.; Muñoz, R.; Guisán, J.M.; Fernández-Lorente, G. Improvement of Enzyme Properties with a Two-Step Immobilization Process on Novel Heterofunctional Supports. *Biomacromolecules* **2010**, *11*, 3112–3117. [[CrossRef](#)] [[PubMed](#)]
30. Escobar, S.; Bernal, C.; Mesa, M. Kinetic study of the colloidal and enzymatic stability of  $\beta$ -galactosidase, for designing its encapsulation route through sol–gel route assisted by Triton X-100 surfactant. *Biochem. Eng. J.* **2013**, *75*, 32–38. [[CrossRef](#)]
31. Perna, R.F.; Tiosso, P.C.; Sgobi, L.M.; Vieira, A.M.; Tardioli, P.W.; Soares, C.M.; Zanin, G.M. Effects of Triton X-100 and PEG on the Catalytic Properties and Thermal Stability of Lipase from Free and Immobilized on Glyoxyl-agarose. *TOBIOJ* **2017**, *11*, 66–76. [[CrossRef](#)] [[PubMed](#)]



© 2019 by the authors. Licensee MDPI, Basel, Switzerland. This article is an open access article distributed under the terms and conditions of the Creative Commons Attribution (CC BY) license (<http://creativecommons.org/licenses/by/4.0/>).